EXPERIMENTAL INVESTIGATION OF RAPIDLY ROTATING TURBULENT DUCT FLOW

G.E. Mårtensson, J. Gunnarsson[*], A.V. Johansson and H. Moberg[†]
Department of Mechanics, KTH
S-100 44 Stockholm, Sweden
gustaf@mech.kth.se

ABSTRACT

Rapidly rotating duct flow is studied experimentally with Rotation numbers in the intervall [0, 1]. To achieve this, in combination with relatively high Reynolds numbers (5000 – 30000 based on the hydraulic radius), water was used as the working medium. Square and rectangular duct cross-sections were used and the angle between the rotation vector and the main axis of the duct was varied. The influence of the rotation on the pressure drop in the duct was investigated and suitable scalings of this quantity were studied.

INTRODUCTION

Knowledge concerning the influence of rotation on the structures of turbulence is of fundamental importance in many applications, *e.g.* centrifugal separators, turbines or cooling channels in rotating machinery, as well as meteorology and oceanography.

In centrifugal separator applications, the flow is subjected to extremely high system rotation rates, the Rotation number being typically around unity. At these high Rotation numbers, relaminarization of turbulent flow may occur near solid walls, for example on the stable side of rotating duct and channel flows.

Experimental data on wall-bounded turbulent flows with system rotation are comparitively scarce. This fact is in part due to the difficulties associated with accurate measurements in rotating frames of reference. Earlier investigations have mainly focused on the influence of the rotation magnitude in orthogonal or axial mode, *e.g.* plane channel flow with spanwise rotation or pipe flow with an axial rotational component. In the present study, the dependance on both the magnitude and the direction of the rotation vector are elucidated. Experimental data were taken for a set of five different rectangular channel geometries, which were investigated for different rotational velocities and different directions of the rotational vector and a range of Reynolds numbers. The Reynolds number was varied between 5000 to 30000, while the Rotation number lay in the interval 0 to 1.

From the data, suitable scalings for the frictional coefficient, using combinations of the Reynolds number and the Rotation number, were extracted for the different experiments.

The effect of rotation on the laminar flow in a straight duct of square section was studied in some detail by Smirnov *et al.* (1983). Through a study of Dobner's (1959) pressure data gathered in a rotating duct, Smirnov states that the drag in a rotating duct is primarily determined by the shear stresses in the horizontal Ekman layers. Hence, the friction coefficient is increased when the flow is subjected to a spanwise rotation.

Johnston *et al.* (1972) performed pioneering work in the field of rotating flows. They investigated the effects of spanwise rotation on fully developed turbulent plane channel flow. By means of hydrogen bubbles and dye-injection, they were able to visualize the suppression of turbulence on the stabilized side of the channel, that is the side where the Coriolis force increases as the wall is approached. Hence, we have a direct analogy with the situation of a stable density stratification. The opposite situation prevails on the other, destabilized, side of the channel. The observations of Johnston *et al.* covered a range of Reynolds numbers between 5500 and 15500 with Rotation numbers up to 0.2, where the Reynolds number, $\mathrm{Re} = U_m D/\nu$, and the Rotation number, $\mathrm{Ro} = 2|\Omega|D/U_m$, and are based on the bulk mean velocity and channel height $2D$, respectively. During the same investigation they observed the development of large-scale roll-

[*] Adtranz, Västerås, Sweden
[†] Alfa Laval, S–147 80 Tumba, Sweden

cells on the destabilized side. The difficulties associated with this kind of flow are acknowledged by the fact that Nakabayashi and Kitoh (1996), limited their investigation to Rotation numbers less than or equal to 0.055, which in their case, with air as working medium, was achieved with a rotation rate of 780 rpm, compared to 14 rpm in the study by Johnston *et al.* Thus, in order to achieve a Rotation number of order one it is of practical necessity to use water or another liquid as working medium.

Launder *et al.* (1987) showed that the qualitative characteristics of fully developed turbulent channel flow with spanwise rotation could be captured with a second-moment closure. Direct numerical simulations of fully developed channel flow with substantial system rotation first appeared in the literature as late as 1993 (Kristoffersen and Andersson). They found good qualitative as well as reasonable quantitative agreement with the experiments by Johnston *et al.* (1972).

A DNS study of rotating channel flow driven by a constant pressure gradient at various Reynolds and Rotation numbers was done by Alvelius and Johansson (2001). The calculations employed a pseudo-spectral code and a long computational domain to ensure accurate results. They found that the streamwise coherence of the elongated roll cell-like structures was particularly accentuated at very low Rotation numbers (Ro = 0.05).

The results of Alvelius (2001) were used as a benchmark in the LES study of Pallares and Davidson (2000), who carried out LES simulations using the localized dynamic subgrid-scale model for low Reynolds number ($\mathrm{Re}_\tau = 300$) duct flow for Rotation numbers in the intervall $0 \leq \mathrm{Ro}_\tau \leq 1.5$. The index τ indicates that the average friction velocity u_τ was used. They obtained results for lower order statistics which are in good qualitative agreement with the DNS data.

THEORETICAL BACKGROUND

Governing equations

The governing equations for an incompressible fluid flow, the Navier-Stokes equations, can in a frame of reference rotating at a constant rate, be written in non-dimensional form as

$$\begin{aligned} \frac{\partial \boldsymbol{u}}{\partial t} + (\boldsymbol{u}\cdot\nabla)\boldsymbol{u} &= -\nabla p_{\mathrm{eff}} + \frac{1}{\mathrm{Re}}\nabla^2\boldsymbol{u} \\ &- 2\mathrm{Ro}(\boldsymbol{k}\times\boldsymbol{u}), \end{aligned} \qquad (1)$$

$$\boldsymbol{k} = \frac{\boldsymbol{\Omega}^{(s)}}{|\boldsymbol{\Omega}^{(s)}|}. \qquad (2)$$

The centrifugal force is included in the pressure term giving the so-called reduced pressure, p_{eff}. The equations have been non-dimensionalized by the bulk velocity, U_b, and the hydraulic diameter, d_h, defined as,

$$U_b = \frac{Q}{w\cdot h}, \qquad d_h = \frac{4(w\cdot h)}{2(w+h)} \ . \qquad (3)$$

Here Q denotes the volume flow, while w and h are the width and the height of the duct, respectively. The Reynolds number and the Rotation number become $\mathrm{Re} = U_b d_h/\nu$ and $\mathrm{Ro} = \Omega d_h/U_b$, respectively. The Ekman number can be formed from the Reynolds and the Rotation number, as $\mathrm{E} = 1/(\mathrm{Re}\cdot\mathrm{Ro})$. The inverse of the Rotation number is often referred to as the Rossby number, ε.

The Coriolis force has a significant effect on the dynamics of the flow, even at low rotation rates. The Coriolis effect on the flow is two-fold in a turbulent duct flow. Primarily, a secondary flow is induced in the mean velocity field. The Coriolis force also affects the structure of the turbulence.

Rotating duct flow

Consider a rectangular duct rotating around the z-axis perpendicular to the main flow, see figure 1. Let $[\, u(y,z),\ v(y,z),\ w(y,z)\,]$ denote the velocity in the fully developed flow at a specific position in the y-z-plane.

The Coriolis force sets up a pressure gradient in the y-direction, so that the main balance in the y-component of equation (1) in the central region of the flow is given by

$$\frac{\partial p_{\mathrm{eff}}}{\partial y} = -2\mathrm{Ro}\,u \ . \qquad (4)$$

In a plane channel with a homogeneous z-direction, this results in the equivalent of a hydrostatic pressure field. In a duct with finite extension in the z-direction, the wall boundary conditions give a spanwise variation of the streamwise velocity that in turn yields a spanwise pressure gradient and a resulting secondary flow in the cross-stream plane. Near the z-boundaries, where the axial velocity, and hence the Coriolis force, is smaller than in the center of the duct, the pressure gradient in equation (4) will drive a flow in the positive y-direction. The resulting secondary flow is illustrated schematically in figure 1.

Near the z-boundaries, we have a turbulent counterpart to Ekman layers. We may consider the region close to the y-boundaries as a turbulent counterpart to the Stewartson layers. We should keep in mind that in the present turbulent case, there is an influence of the Reynolds stresses on the secondary flow.

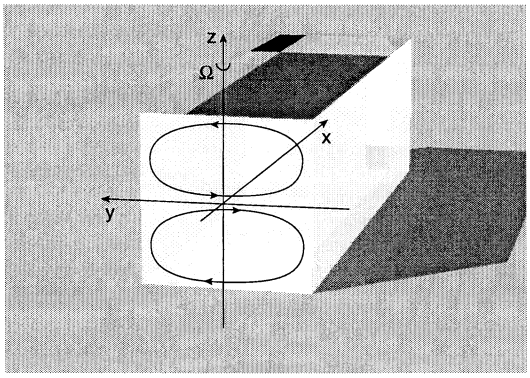

Figure 1: The secondary flow in a rotating square duct.

The laminar Ekman and Stewartson layer thicknesses scale as $E^{\frac{1}{2}}$ and $E^{\frac{1}{3}}$ or on dimensional form, $\delta_E \sim \sqrt{\nu d_h/\Omega}$, $\delta_S \sim (\nu d_h/\Omega)^{\frac{1}{3}}$. There can also exist secondary Stewartsson layers whose thicknesses scale as $\delta_{S'} \sim E^{\frac{1}{4}}$.

In requiring the vertical Ekman layers to carry the same mass flux as the horizontal Stewartson layers, it is obvious that the major contribution to the total wall shear, and thereby flow resistance, originates from the Ekman layers in this range of Rotation numbers. The situation is of course modified in a turbulent case, but it is reasonable to expect that the increase in friction coefficient will scale approximately with the width of the duct, rather than with the hydraulic diameter.

Inclined rotating duct

Let us assume a fully developed turbulent flow ($\frac{\partial}{\partial x} = 0$) in a rectangular duct with system rotation vector $\mathbf{\Omega} = \Omega(k_x, 0, k_z)$, see figure 1. The Coriolis term in the momentum equation (1) then becomes

$$-2\mathrm{Ro}(-k_z v, k_z u - k_x w, k_x v) \quad , \qquad (5)$$

from which we note that the axial component of the rotation (k_x) only multiplies the secondary velocity components. Since the mean streamwise velocity fluctuations are much larger than the cross-stream velocity fluctions, one may argue that only small effects from the axial rotation component are to be expected. However, the turbulence modifying effects can be large since all the fluctuating components may all have magnitudes of the same order locally. The Coriolis term has a direct influence on the transfer between the Reynolds stress components, as can be seen from the Reynolds stress transport equations in a rotating frame of reference. For instance, these effects give rise to the secondary swirl in axially rotating turbulent pipe flow, see for example Ito *et al.* (1971). No previous experiments or simulations on an inclined rotating duct are known to the authors.

EXPERIMENTAL APPARATUS

In an attempt to simplify a very complex physical system that for example an industrial separator consists of, while at the same time retaining the essential physical properties and problems therein, a rotating rectangular duct was chosen.

The experimental setup is illustrated schematically in figure 2. The overall channel length was 490 mm, giving a ratio of length to hydraulic diameter of between 30 – 47, depending on the choice of duct. It is customary to try to achieve a length to height ratio of at least 50 in experiments on pipe or duct flow to guarantee a fully developed profile. A length to height ratio of 32 was used by Johnston *et al.* (1972). The inlet length required can be shortened by introducing disturbances at the inlet. Also, rotation may help somewhat in this respect.

In order to obtain high Rotation numbers in combination with high Reynolds numbers, water was chosen as flow medium. The highest rotation rate used in the present investigation was approximately 25 rad/s.

A converging nozzle was used to form a smooth transition from the circular pipe to the rectangular ducts. Screens made of stainless steel wires were mounted before and after the inlet nozzle to break up large structures and to give a suitable level of inlet disturbances. The screen configuration was chosen to give a pressure drop similar to that for the duct flow.

Re	5000 – 30000				
Ro	0 – 1.0				
α	45°	60°	75°	90°	
A	1/1	2/3	3/2	1/3	3/1
$w \times h$	15 × 15	14 × 21	21 × 14	7 × 21	21 × 7

Table 1: Parameter range of the experiment ($A = w/h$, w and h in millimeters).

To achieve a rotation vector that is not perpendicular to the direction of the main flow, a

construction with four interchangeable middle sections was used. The angle between the axis of rotation and the longitudinal axis could in this way be altered in four discrete steps (90°, 75°, 60° and 45°). The construction was machined from solid aluminium in order to obtain the rigidity to withstand the dynamic forces due to the asymmetry of the construction.

A total of five different duct geometries were used during the experiments, see table 1, giving a total of twenty (20) different possible configurations, for each combination of Reynolds and Rotation numbers.

Pressure holes with a diameter of 0.5 mm were placed at 10 cm intervals along the duct centerline. The pressure drop was measured using a differential pressure transducer. The pressure transducer was mounted on the axis of rotation, see figure 2. Conventional tubing was used to connect the pressure holes to the transducer. In this way, the pressure induced by the centrifugal force is automatically subtracted from the sampled pressure signal. Positioning the pressure tranducer in this manner will also minimize the imposed structural stresses by minimizing the moment of inertia. The membrane has a finite width and will therefore be affected by the rotation, but since the the centrifugal force is parallel to the membrane surface these effects are considered to be negligible. The signal from the pressure transducer was transmitted from the rotating frame via a slip-ring device.

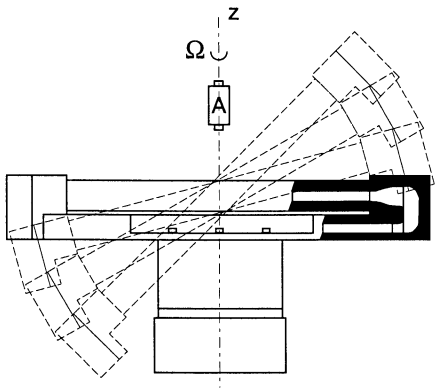

Figure 2: Schematic of the experimental apparatus. The pressure transducer is labeled **A**.

RESULTS

For a stationary pipe, the friction factor is approximately given by the empirical formula,

$$\lambda_0 = 0.3164\,\mathrm{Re}_d^{-\frac{1}{4}}, \quad 4\cdot 10^3 \leq \mathrm{Re}_d \leq 10^5 \quad . \quad (6)$$

The friction coefficient for a non-circular duct can be calculated as $\lambda_{\mathrm{non-c}} = k_{\mathrm{non-c}}\lambda_{\mathrm{pipe}}$, where the correction factor $k_{\mathrm{non-c}}$ for a rectangular duct has been tabulated by *e.g.* Idelchik (1986), see table 2.

a/b	0	0.1	0.2	0.4	0.6	0.8	1.0
$k_{\mathrm{non-c}}$	1.10	1.08	1.06	1.04	1.02	1.01	1.00

Table 2: Correction factor $k_{\mathrm{non-c}}$ for turbulent flows in rectangular ducts Idelchik (1986), pp. 87.

A more accurate formulation of the friction coefficient for ducts is given by Jones (1976)

$$\frac{1}{\sqrt{\lambda_0}} = 2\log \mathrm{Re}_j \sqrt{\lambda_0} - 0.8\ , \quad (7)$$

where Re_j is a modified bulk Reynolds number. For a square duct, $\mathrm{Re}_j = 1.125\,\mathrm{Re}$ was proposed. Gavrilakis (1992) obtained good agreement with this formula in a DNS study of square duct flow. The present data give a friction coefficient that is approximately 5% lower than that given by the Jones formula.

To isolate the dependence of the system rotation, the friction coefficient for the rotating system in the following is normalized using the friction coefficient for the inertial system. We investigate the possibility of collapsing the friction factor results for different geometrical aspect ratios, Reynolds numbers and Rotation numbers onto a single curve.

Square duct

From the empirical formulas of Blasius and Jones for stationary ducts, equations (6) and (7), we know the friction coefficient to be a function of the Reynolds number, $\lambda_0 = \lambda_0(\mathrm{Re})$. For the rotating duct, we may assume that the friction coefficient should be a function of the Rotation number, as well as the Reynolds number, $\lambda = \lambda(\mathrm{Re}, \mathrm{Ro})$. Results from measurements on the square duct are presented in figure 3. We see that the normalized friction coefficient nearly collapse onto one line when plotted against the parameter Ro/Re.

From the measurements performed with the square channel (15×15 mm^2), a monotonic increase of the friction factor is observed with increasing Rotaion number.

To further probe the importance of the geometrical configuration of the duct, the case of the tilted duct was studied. The channel was tilted 45° around its longitudinal axis. If the square duct is tilted in this way, the friction coefficient increases more rapidly with the rotation rate, see figure 5 a). One possible

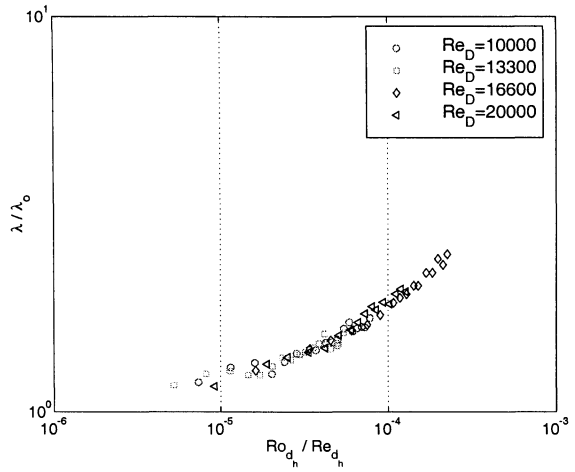

Figure 3: Normalized friction loss coefficient for 15mm × 15mm duct, ○: $Re_D = 10000$, □: $Re_D = 13300$, ◇: $Re_D = 16600$, ⋆: $Re_D = 20000$

explanation of this is that instead of the standard configuration of two Stewartsson layers and two Ekman layers of the untilted case, four Ekman layers are formed on the walls of the tilted duct. This is believed to be a geometric effect, since when there are no vertical walls the formation of Stewartson layers is inhibited.

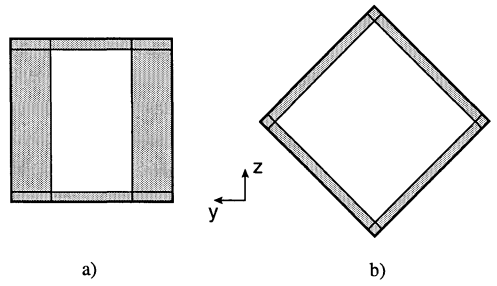

Figure 4: By tilting the duct 45° around the streamwise axis, four Ekman layers may be formed, intsead of two in the case of a non-tilted channel.

The wall shear stress in a boundary layer may be taken to be proportional to the inverse of the boundary layer thickness. With a scaling of the thickness as $E^{\frac{1}{2}}$, the local wall shear stress should decrease as $(\sin\beta)^{\frac{1}{2}}$, where β is the tilting angle, since the wall normal rotation rate becomes $\Omega \sin\beta$. The total length however is doubled, so for $\beta = 45°$, we should expect an increase in pressure drop by a factor $2/\sqrt[4]{2}$. This factor is dependant on the assumption that in the non-tilted case, the two Ekman layers are the dominant contributors to the total pressure drop in the duct.

The collapse of data is good if this scaling is applied to the available data, see figure 5. The agreement is better for higher rotation rates which is in line with the reasoning above.

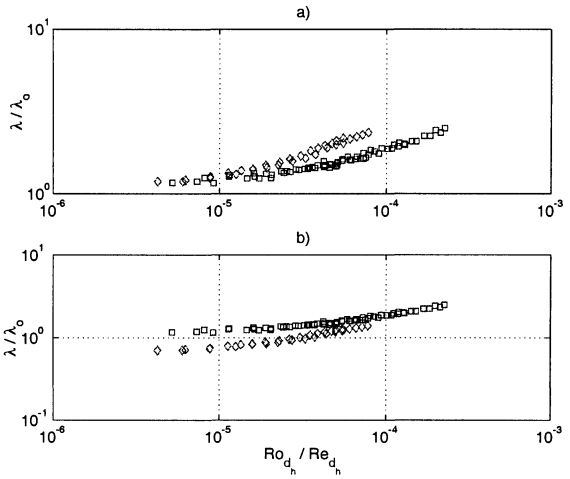

Figure 5: Normalized friction coefficient for a duct tilted by 45° (□) and a non-tilted duct (○). In a), the the normalised friction coefficient has been plotted as measured in the two cases, while in b), the data from the tilted channel has been adjusted by a factor $2/\sqrt[4]{2}$.

Square inclined duct

If the turbulent duct flow is subjected to a rotation other than one that is orthogonal, see figure 2, the friction coefficient will increase at a slower pace. The effect of the axial rotation component, $\Omega_x = \Omega \cos\alpha$, which can be expected to stabilize the flow (*cf.* axially rotating pipes), turns out to be small in comparison to the effect of the orthogonal component $\Omega_z = \Omega \sin\alpha$. Thus, we may define reduced Rotation and Ekman numbers (Ro_α, E_α) respectively, with this rotation rate.

In figure 6, the normalized friction coefficient for a square duct in its different angular configurations is plotted versus the parameter $\mathrm{Ro}_\alpha/\mathrm{Re}$. One should note that the normalised friction coefficient dat coincides with those for the duct rotating in orthogonal mode. This leads us to conclude that, at least for these angles of rotation, the effect of the normal rotation component is completely dominant.

Rectangular duct

In analysing the data from the measurements of the rectangular ducts, we are guided by the discussion earlier concerning the dominance of the Ekman layer's influence on the pressure drop along the length of the channel.

If the normalised friction coefficient is plotted versus the parameters Ro_h and Ro_w, where the indices h and w imply that the characteristic lengths were chosen as the height and the width of the channel geometry, respectively, we observe a far better collapse of the data for those plotted versus Ro_w, see figure 7.

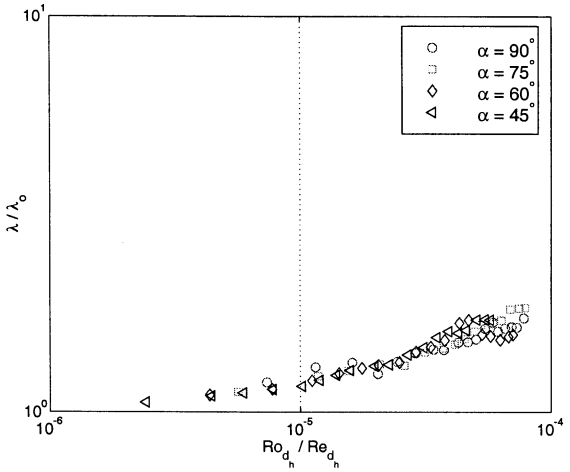

Figure 6: Normalized friction loss coefficient for 15 mm × 15 mm duct, $Re_D = 10000$, o: $\alpha = 90°$, □: $\alpha = 75°$, ◇: $\alpha = 60°$, ◁: $\alpha = 45°$

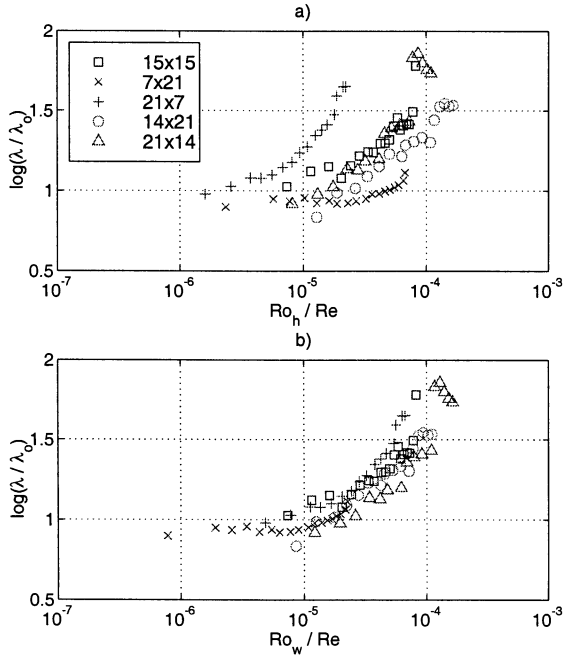

Figure 7: Normalized friction loss coefficient versus the Rotation number for Re = 10000. In a), the characteristic length for the Rotation number is chosen as the height of the channel, while in b), this length is chosen as the width of the channel. ($w \times h$) □: 15 × 15, ×: 7 × 21, +: 21 × 7, o: 14 × 21, △: 21 × 14.

CONCLUSIONS

The effect of rotation on turbulent flow was studied by measuring the pressure drop in a rotating rectangular duct for a number of configurations of Rotation and Reynolds numbers. The friction coefficient was found to increase with the Rotation number. By studying the inclined duct flow, it was fortified that it is the normal component of the rotation vector that is of primary importance in understanding the effect of rotation on this kind of flow.

The study of several duct geometries revealed that the contribution to the pressure drop by the equivalent Ekman layers is dominant in the duct, yielding the width of the duct as the important characteristic length.

REFERENCES

Alvelius, K, and Johansson, A.V., 2001, "Direct numerical simulation of rotating channel flow at various Reynolds numbers and Rotation numbers", submitted to *J. Fluid Mech.*

Dobner, E., 1959, "Über den Strömungswiderstand in einem rotirenden Kanal", Dissertation, Technische Hochschule Darmstadt.

Gavrilakis, S., 1992, "Numerical Simulation of low-Reynolds-number turbulent flow through a straight square duct", *J. Fluid Mech.*, **244**, 101–129.

Idelchik, I.E., "Handbook of hydraulic resistance", *Springer-Verlag*, 1986.

Ito, H. and Nanbu, K., 1971, "Flow in Rotating Straight Pipes of Circluar Cross Section", *Trans. ASME - J. Basic Eng.*, **93**(3), 383–394.

Johnston, J.P., Halleen, R.M. and Lezius, D.K., 1972, "Effects of spanwise rotation on the structure of two-dimensional fully developed turbulent channel flow", *J. Fluid Mech.*, **56**, 533–557.

Jones, O.C., 1976, "An improvement in the calculation of turbulent friction in rectangular ducts", *Trans. ASME* J: *J. Fluid Engng*, **98**, 173–181.

Kristoffersen, R. and Andersson, H.I., 1993, "Direct simulations of low-Reynolds-number turbulent flow in a rotating channel", *J. Fluid Mech*, **256**, 163-197.

Launder, B.E., Tselepidakis, D.P. and Younis, B.A., 1987 "A second-moment closure study of rotating channel flow", *J. Fluid Mech.*, **183**, pp. 63–75

Nakabayashi, K. and Kitoh, O., 1996, "Low Reynolds number fully devloped two-dimensional turbulent channel flow with system rotation", *J. Fluid Mech.*, **315**, 1–29.

Pallares, J., and Davidson, L., 2000, "Large-Eddy Simulations of turbulent flow in a rotating square duct", *Phys. Fluids*, Vol. 12, No. 11, pp. 2878 – 2894.

Smirnov, E.M. and Yurkin, S.V., 1983, "Fluid flow in a rotating channel of square section", *Fluid Dyn.*, **18**(6), 850–855.